

# Optimal Network Tariffs for Renewable Electricity Generation\*

(Work in progress - Preliminary and incomplete)

Thomas P. Tangerås<sup>†</sup> and Frank A. Wolak<sup>‡</sup>

May 23, 2017

## Abstract

The intermittency (variability) of solar and wind power imposes network costs associated with maintaining system stability. We examine how the socially optimal deployment of intermittent renewable generation capacity depends on such ancillary services costs and demonstrate how network interconnection tariffs can be designed to implement the efficient outcome. We then apply our theory to obtain quantitative results for the California electricity market.

Key words: Ancillary services costs, efficiency, network tariffs, renewable electricity production, system stability.

JEL: L94, Q20, Q42

---

\*This research was conducted within the "Economics of Electricity Markets" research program at IFN. Financial support from the Swedish Energy Agency is gratefully acknowledged. Financial support from the Department of Energy is also gratefully acknowledged.

<sup>†</sup>Research Institute of Industrial Economics (IFN) P.O. Box 55665, 10215 Stockholm, Sweden, e-mail: thomas.tangeras@ifn.se.

<sup>‡</sup>Program on Energy and Sustainable Development and Department of Economics, Stanford University, 579 Serra Mall, Stanford, CA 94305-6072, e-mail: wolak@zia.stanford.edu

# 1 Introduction

The intermittency (variability) of solar and wind power imposes costs on the grid associated with maintaining system stability and reliability. Examples of such *ancillary services costs* include automatic generation control (AGC), spinning reserves, non-spinning reserves, and fast ramping reserves. Historically, the share of intermittent renewable generation capacity in most jurisdictions was small, which meant that allocating ancillary services costs across consumers and/or producers in an arbitrary manner did not result in significant economic efficiency losses. However, in many regions ancillary services costs have become increasingly important with the surge in intermittent renewable energy production brought about by renewable energy mandates.

In California, for example, annual ancillary services costs as a share of total wholesale energy costs more than doubled from 2015 to 2016.<sup>1</sup> The California Independent System Operator (ISO) also more than doubled its average hourly regulation reserve (AGC) requirement between 2015 and 2016. The primary driver of these changes was almost 2,000 megawatts (MWs) of new grid scale solar generation capacity coming on line during 2016. California has a 33% percent renewable portfolio standard (RPS) by 2020 and a 50% RPS by 2030, so ancillary services quantities and ancillary services costs are likely to become an even larger share of total wholesale energy costs in the future.

These trends in ancillary services quantities and costs are common to all regions with significant intermittent renewable energy goals. They provide strong evidence that the economic efficiency consequences of continuing to allocate ancillary services costs in an arbitrary manner are increasing. One way of internalizing ancillary services costs is through network interconnection tariffs that price locational differences in the factors driving these costs. Specifically, different dollar per MW of capacity installed interconnection tariffs would be assessed for intermittent renewable resources interconnecting at different renewable resource locations in the transmission grid. Keeping other factors the same, this tariff should encourage interconnection at locations that minimize the adverse market efficiency consequences of meeting a region's intermittent renewable energy goals.

This paper characterizes the socially efficient expansion of intermittent renewable generation capacity needed to achieve a specified renewable energy target (such as California's 33 percent renewable energy goal) in a manner that accounts for the reliability externality associated with the necessary intermittent generation investments. By subtracting the first-order condition for a generation unit owner's capacity expansion decision at a location in the grid and the first-order conditions from our socially optimal investment solution at that same location, we derive an expression for the dollars per MW marginal interconnection charge that could implement the social optimum as decentralized market outcome. We then use market outcome and hourly generation data from the California ISO control area to estimate features of the joint distribution of hourly capacity factors

---

<sup>1</sup>California Independent System Operator, 2016 Annual Report on Market Performance and Issues, p. 141, available at <https://caiso.com/Documents/2016AnnualReportonMarketIssuesandPerformance.pdf>

for all renewable resource areas in California and the other parameters of our model necessary to compute values of the locational interconnection charges. Based on those estimates, we compute two socially efficient investment solutions (one constraining investment at each location to be at least the current capacity at that location and the other only requiring non-negative capacities at all locations) and the optimal locational interconnection charges associated with them. Finally, we compute several alternative solutions to achieving California’s renewable energy goals and compare the costs of attaining those goals under these solutions to the costs under our two efficient solutions.

The social planner’s problem is how to distribute incremental or total intermittent capacity across renewable resource locations in a control area so as to maximize total surplus, subject to an annual output target for renewable energy production. This problem is very similar to a portfolio selection problem in which a manager distributes investment dollars across financial assets to minimize the variance of returns subject to achieving a minimal expected return. There are two major differences between the classical portfolio choice and the renewable generation investment problems. First, short sales are impossible because capacity at each location must be non-negative. In the incremental capacity expansion problem, existing capacity at that location is sunk. Second, the optimal renewable generation capacity investment portfolio depends on factors other than the variance and covariance of outputs, for instance the covariance with consumption. This second feature is likely to be important in reality because some intermittent generation technologies are better suited to meet peak demand than others. For example, in California solar generation capacity produces the most energy during daylight hours versus wind generation capacity that tends to produce more energy in the early morning and late evening hours.

We find significant differences across locations in the value of the optimal interconnection tariffs for California renewable generation locations. Although the absolute level of the tariffs are modest, less than one dollar per MW of installed capacity for each hour of the year, they differ by multiples as high as four to one across California renewable resource locations. We also find that plausible counterfactual renewable generation capacity expansion paths to achieve the 33% renewable energy goal lead to significantly higher total costs of meeting the RPS. Our empirical results demonstrate the feasibility and effectiveness of implementing location-specific renewable generation capacity interconnection tariffs for regions with ambitious renewable generation capacity expansion goals.

The remainder of the paper proceeds as follows. Section 2 characterizes the growing renewable generation intermittency challenge facing California. Section 3 presents our theoretical modeling framework and derives the socially optimal renewable energy investment solution for meeting a given renewable energy goal. This section then uses this modeling framework to derive the optimal locational renewable resource interconnection tariff. Section 4 contains our application to the California electricity market and derives two social solutions to meeting California’s 33 percent RPS along with the optimal locational renewable resource interconnection tariffs. Section 5 considers several counterfactuals that illustrate the increased cost of meeting California’s RPS goal using plausible non-optimal policies for intermittent renewable generation capacity expansion. Section 6

concludes the paper with a brief policy discussion.

## 2 California's Renewable Generation Challenge

California has invested in over 6,500 MW in grid-scale solar generation capacity and over 4,400 MW of grid-scale wind generation capacity between 2002, when the state's RPS was first implemented, and the end of 2015.<sup>2</sup> For solar capacity, virtually all of this investment has taken place since 2011, whereas for wind this investment has occurred at a steady annual rate since 2002. As of the beginning of 2016, there was almost 7,000 MW of solar generation capacity and almost 6,000 MW of wind capacity in California. However, average hourly wind and solar energy produced in 2016 is significantly lower. More than fifty percent of the hours in 2016, hourly wind output was less than 1,500 MWh and hourly solar output was less than 1,000 MWh. For combined wind and solar output, more than fifty percent of the hours of the year hourly output was less than 2,500 MWh.

Figure 1 plots the histogram of hourly wind output in the California ISO control area for 2016 conditional on a positive value of hourly wind output. The expression  $P(\text{TotalOutput}=0)$  at the bottom of Figure 1 is equal to the fraction of hours in the year with zero wind output—approximately 1 percent of the hours in 2016. This histogram is extremely skewed to the right and has a substantial amount of frequency mass close to zero hourly output. The histogram rapidly decreases to zero frequency more than 2,000 MWh below the installed capacity of wind units in the state.

Figure 2 plots the histogram of hourly solar output for 2016 conditional on a positive value of hourly solar output. As shown at the bottom left of the figure, in more than 45 percent of the hours in 2016 hourly solar output was equal to zero. This histogram is bimodal, with one peak very close to zero and another smaller peak close to 5,000 MWh. With the exception of very low hourly output levels, the distribution of hourly solar output levels is relatively flat across all output levels. Different from the case of wind capacity, there are a number of hours in 2016 when the hourly solar output was very close to the amount of installed solar generation capacity in the California.

Figure 3 plots the histogram of the sum of hourly wind and solar output for 2016 conditional on this sum being positive. Approximately 0.4 percent of the hours in 2016 no wind nor solar energy was produced. This histogram is tri-modal, with the largest frequency at very low levels of hourly output. There is second spike at 2,000 MWh and another smaller one at 6,000 MWh. This histogram also has a very significant right skew.

How have this distribution changed over time as California has expanded the amount of solar and wind generation capacity? One might expect that as more renewable resource locations are developed, the uncertainty in hourly wind, solar, and wind and solar output should decline. This intuition is based on the logic that there is little contemporaneous correlation between hourly renewable energy output at different resource locations in California. However, as shown in Wolak

---

<sup>2</sup>California Energy Commission—Tracking Progress available at [http://www.energy.ca.gov/renewables/tracking\\_progress/documents/installed\\_capacity.pdf](http://www.energy.ca.gov/renewables/tracking_progress/documents/installed_capacity.pdf)

(2016), there is a substantial amount of contemporaneous correlation between the hourly output of solar locations in California and hourly output of wind locations in California.

Wolak (2016) uses one year of hourly output data from all wind and solar units in California between April 1, 2011 and March 31, 2012 and computes the capacity factor  $f_{jh}$  at location  $j$  during hour  $h$  for all hours of the year as  $f_{jh} = \frac{Q_{jh}}{K_j}$ , where  $Q_{jh}$  is the hourly output in MWh at renewable energy location  $j$  during hour  $h$  and  $K_j$  is the amount of renewable generation capacity in MW at location  $j$ . Wolak (2016) then computes the contemporaneous covariance matrices of the hourly capacity factors of all 13 solar locations, all 40 wind location and all 53 wind and solar locations that existed during his same period. He then performs an eigenvalue decomposition of these covariance matrices and finds that more than 80 percent of the sum of variances in hourly capacity factors across the 13 solar locations can be explained by a single factor. For the 40 wind locations, more than 80 percent of the sum of the variances in the hourly capacity factors across these locations can be explained by three orthogonal factors. For the 53 wind and solar locations, more than 80 percent of the sum of the variances in the hourly capacity factors across these locations can be explained by 5 orthogonal factors.

Wolak (2016) argues that these results demonstrate that adding more renewable generation capacity in California is likely to increase significantly the aggregate uncertainty in renewable energy output. To demonstrate this point, Wolak (2016) uses parameterized expressions for the mean and covariance of the vector of hourly capacity factors across all renewable energy locations to compute the efficient frontier of portfolios of renewable generation capacity investments with the same total installed capacity of wind and solar generation units in California, but with every portfolio on this efficient frontier having the largest mean hourly capacity factor for the given portfolio standard deviation of the hourly capacity factor. The actual portfolio of wind and solar generation units in California is shown to lie significantly inside this efficient frontier, which indicates the significant potential reliability and economic benefits of locational interconnection pricing as a mechanism for the reducing the variability in aggregate hourly renewable output and the costs of managing system reliability.

Table 1 reports the annual mean, standard deviation, Coefficient of Variation (CV), standardized skewness, and standardized kurtosis of the hourly wind, solar and combined wind and solar output for 2013 to 2016.<sup>3</sup> Standard deviations increase across all years and all three types of hourly output. This is consistent with the amount of installed renewable generation capacity increasing across the years. The sample CV provides a normalized measure of the variability in the three hourly output measures that accounts for the growth in the annual mean hourly output across the years. Consistent with the results reported in Wolak (2016), the general trend is that CV increases across the years. The standardized skewness of the annual distribution of hourly output of wind

---

<sup>3</sup>If  $X_h$  is the output in hour  $h$ ,  $\bar{X}$  is the annual mean of hourly output and  $s$  is the annual standard deviation of hourly output, then the Coefficient of Variation is equal to  $s/\bar{X}$ , the standardized skewness is equal to  $1/H \sum_{h=1}^H (X_h - \bar{X})^3 / s^3$ , and the standardized kurtosis equals  $1/H \sum_{h=1}^H (X_h - \bar{X})^4 / s^4$ , where  $H$  is the number of hours in a year.

and solar resources also increases across the years.

Another measure of intermittency that signals the need for system operators to purchase more ancillary services as the share of intermittent renewable resources increases is the duration of low hourly renewable output levels. For each year from 2013 to 2016, we choose an hourly output level, say 500 MWh, and then starting with the first hour of January 1 of the year, we look for the first hour that has an hourly output of wind, solar, or wind and solar energy production below this level. Then we count how many consecutive hours the hourly output remains below this level. This counts as one duration of low output levels below the 500 MWh threshold and then we record the length of this duration in hours. We repeat this same process of finding spells of hourly output less than 500 MWh for all hours of the year. Table 2 reports the number of durations of low hourly output of wind for 500, 100, 1,500 and 2,000 MWh threshold values. The length of these durations in hours and the standard deviation of these durations, as well as the maximum length duration is reported. Particularly, for the earlier years in the sample, there are extremely long maximum periods of low renewable output. Even by 2016, when there is almost 6,000 MW of wind capacity in California, the maximum duration of less than 2,000 MWh of wind output was 399 hours, which is more than 16 days.

Table 3 reports Table 2 for solar output. The maximum duration of low levels of solar output are significantly smaller than those for wind output. Table 4 reports Table 2 for the combined hourly wind and solar output for 1,000, 2,000, 3,000, and 4,000 MWh hourly output thresholds. Comparing the 1,000 and 2,000 MWh threshold mean duration, standard deviation, and maximum value in Table 4 to those in Tables 2 and 3 demonstrates that combining these two sources of renewable energy reduces the mean duration of low output levels and maximum duration of low output levels relative to the solar or wind alone. However, there are still substantial durations of low output levels that battery storage technologies would have a difficult time dealing with. For example, in 2016 although there is more than 13,000 MW of wind and solar capacity in California, the maximum duration of less than 4,000 MWh of output from these units was 178 hours, which is more than one week.

These results provide empirical support for the California ISO's increasing demand for ancillary services as the state has scaled up its wind and solar generation capacity. Further evidence for the increased demand for ancillary services and dispatchable generation capacity is the fact that between 2002 and the end of 2015, California has added slightly more natural gas-fired generation capacity, 11,573 MW, than renewable generation capacity, 10,993 MW. Figure 4 plots the installed capacity in California by technology as of the end of the years from 2001 to 2015. Although wind and solar investments have made up virtually all of the capacity additions since 2011, there is still substantial amount of natural gas-fired capacity in California.

The above analysis distribution of the hourly output and wind and solar generation units in California argues that a significant fraction of this thermal capacity will continue to be needed to provide ancillary services and energy as California brings on line more renewable generation units to

meet its RPS goals. These thermal units must be fully compensated for the services they provide or their owners are likely to take them mothball or retire the units, and these costs must ultimately be paid by electricity consumers. Our analysis of optimal renewable generation interconnection pricing is aimed at minimizing these thermal energy and ancillary services costs associated with meeting California's RPS goals.

### 3 Optimal Renewable Generation Investment and Tariffs

#### 3.1 Modeling Renewable Generation Investment

Consider a control area with  $J$  possible locations of intermittent electricity production. This energy typically comes from wind and solar generation capacity. Denote by  $K_j$  the installed intermittent generation capacity at location  $j$ , measured in megawatts (MW), with  $\mathbf{K} = (K_1, K_2, \dots, K_J)'$  being the  $J \times 1$  vector of intermittent generation capacity at all possible locations. Let  $Q_{jh}$  be the amount of electricity actually produced at location  $j$  during hour  $h = 1, 2, \dots, H$ , where  $H$  is the total number of hours in the year.

Define  $f_{jh} = Q_{jh}/K_j$  as the hourly capacity factor at location  $j$  during hour  $h$ , i.e. actual production at location  $j$  during hour  $h$  divided by the amount that could be produced by full utilization of the  $K_j$  MWs of capacity at that location. Let  $\mu_j$  be the expected value of  $f_{jh}$ . The corresponding vector of realized capacity factors during hour  $h$  is equal to  $\mathbf{f}_h = (f_{1h}, f_{2h}, \dots, f_{Jh})'$ , and the expected value of  $\mathbf{f}_h$  is equal to  $\boldsymbol{\mu} = (\mu_1, \mu_2, \dots, \mu_J)'$ . Also, define the  $J \times J$  (positive definite) covariance matrix  $\boldsymbol{\Sigma} = E[(\mathbf{f}_h - \boldsymbol{\mu})(\mathbf{f}_h - \boldsymbol{\mu})']$ . Let  $\sigma_{ij}$  be the  $(i, j)$ th element of  $\boldsymbol{\Sigma}$ . We assume that these moments are constant across  $H$ .

In terms of this notation, the actual output during hour  $h$  at location  $j$ ,  $Q_{jh}$ , is equal to  $f_{jh}K_j$ , and the expected output,  $E[Q_{jh}]$ , is equal to  $\mu_j K_j$ . Total renewable energy output during hour  $h$  therefore equals  $R_h = \sum_{j=1}^J Q_{jh} = \mathbf{f}_h' \mathbf{K}$ , and the expected renewable energy output is  $E[R_h] = \boldsymbol{\mu}' \mathbf{K}$ . The variance of hourly renewable energy production is equal to  $\mathbf{K}' \boldsymbol{\Sigma} \mathbf{K}$ . Let  $QD_h$  be the realized value of system demand during hour  $h$  and  $E[QD_h]$  its expected value.

The difference between system demand  $QD_h$  and the intermittent renewable electricity production  $R_h$  during hour  $h$ , yields a residual demand that must be covered by dispatchable generation capacity, primarily thermal generation units. Let  $C^h(R_h, QD_h)$  be the total variable cost of serving this residual demand during hour  $h$ . In addition, there is an ancillary services cost  $A^h(R_h, QD_h)$  associated with maintaining system stability. Let  $C^h(R_h, QD_h)$  and  $A^h(R_h, QD_h)$  be convex in  $R_h$ . Assume also that the total amount of thermal generation capacity and transmission network capacity are sufficiently large and intermittent electricity production sufficiently small relative to these capacities that neither demand nor renewable output has to be curtailed.

Under the assumption that all of the random variables—the elements of the vector  $\mathbf{f}_h$  and  $QD_h$ —have the same first two moments across years, the expected net present value (ENPV) of investing

one MW of capacity at location  $j$  equals:

$$\sum_{t=1}^{\tau} \sum_{h=1}^H \delta^t E[pr_{jh}f_{jh} - \frac{S^j(\mathbf{K})}{K_j}] - F_j, \quad (1)$$

where  $\tau$  is the life-span of the investment and  $\delta$  the annual discount rate. The price  $pr_{jh}$  paid per unit of renewable output at location  $j$  during hour  $h$  typically contains a subsidy to the renewable resource owners and therefore can differ substantially from the wholesale price  $p_{jh}$ . Often, renewables receive an additional payment per MWh produced that is fixed for the entire term of the power purchase agreement used to finance the construction of the facility:  $pr_{jh} = p\mu_j$  for all  $h$ .

We assume that investors treat  $pr_{jh}$  as exogenous when making their investment decision. We introduce the term,  $S^j(\mathbf{K})/K_j$  into (1) to account for our proposed hourly interconnection tariff paid per unit of capacity installed at that location by the producer for generation unit at location  $j$  in the grid. We allow this charge to depend on the installed capacity  $\mathbf{K}$  at all locations in the grid. Finally,  $F_j$  is the capital cost per MW of capacity, which encompasses the (overnight) construction cost, the cost of connecting the plant to the grid plus the discounted expected overhead and maintenance costs over the life-span of the plant. The investment is undertaken if and only if it has a non-negative ENPV. Let all payments during the  $H$  hours of year  $t$  be made at the end of the year. Normalize the capital cost at location  $j$  to

$$DF_j = \frac{F_j}{H} \frac{1 - \delta}{\delta(1 - \delta^\tau)}$$

and let  $\mathbf{DF} = (DF_1, DF_2, \dots, DF_J)'$  be the vector of normalized capital costs across all  $J$  locations. By this normalization, the average hourly ENPV of investing  $K_j$  MW of renewable capacity at location  $j$  equals

$$\frac{1}{H} \sum_{h=1}^H E[pr_{jh}f_{jh}K_j - DF_jK_j - S^j(\mathbf{K})]. \quad (2)$$

### 3.2 The Efficient Portfolio of Renewable Generation Capacity

To determine the function form of the per MW installed hourly locational interconnection charge  $S^j(\mathbf{K})$ , we first solve the social planner's problem and compare it to the one facing the private investor. The social planner minimizes the sum of expected thermal energy costs, ancillary services costs and renewable generation investment costs,

$$\frac{1}{H} \sum_{h=1}^H E[C^h(R_h, QD_h) + A^h(R_h, QD_h a)] + \mathbf{DF}'\mathbf{K}, \quad (3)$$

subject to the renewable portfolio standard (RPS),

$$\boldsymbol{\mu}'\mathbf{K} \geq \alpha \frac{1}{H} \sum_{h=1}^H E(QD_h), \quad (4)$$

which requires that the expected annual hourly renewable energy production be greater than or equal to  $100\alpha$  ( $0 < \alpha < 1$ ) percent of expected annual hourly electricity demand.

Depending on the problem, we impose the constraint that the installed capacity at location  $j$  must be greater than or equal to zero,  $K_j \geq 0$ , or the installed capacity at location  $j$  be greater than or equal to the existing capacity  $K_j^e$  at location  $j$ ,  $K_j > K_j^e$ . Let  $\mathbf{K}^e$  be the vector of existing capacity at all renewable locations.

The Lagrangian for the social planner's problem where investment at all locations must be greater than or equal to the existing capacity at that location is:

$$\begin{aligned} L(\mathbf{K}, \lambda, \boldsymbol{\xi}) = & -\frac{1}{H} \sum_{h=1}^H E[C^h(R_h, QD_h) + A^h(R_h, QD_h)] - \mathbf{D}\mathbf{F}'\mathbf{K} \\ & - \lambda[\alpha(\frac{1}{H} \sum_{h=1}^H E(QD_h)) - \boldsymbol{\mu}'\mathbf{K}] + \boldsymbol{\xi}'(\mathbf{K} - \mathbf{K}^e) \end{aligned} \quad (5)$$

where  $\lambda \geq 0$  is the Kuhn-Tucker (KT) multiplier associated with the RPS constraint,  $\xi_j \geq 0$  is the KT multiplier associated with  $(K_j - K_j^e) \geq 0$ , and  $\boldsymbol{\xi}$  is the vector of KT multipliers associated with capacity investment constraints at the  $J$  renewable resource locations. This is a strictly concave optimization problem, which allows us to state Proposition 1:

**Proposition 1** *The efficient portfolio  $\mathbf{K}^*$  of renewable generation capacity, the shadow price  $\lambda^*$  on the renewable target, and the shadow prices  $\boldsymbol{\xi}^*$  at the  $J$  locations are jointly characterized by the  $J$  first-order conditions*

$$-\frac{1}{H} \sum_{h=1}^H E \left[ \left[ \frac{\partial C^h(R_h^*, QD_h)}{\partial R_h} + \frac{\partial A^h(R_h^*, QD_h)}{\partial R_h} \right] f_{jh} \right] - DF_j + \lambda^* \mu_j + \xi_j^* = 0, \quad \forall j, \quad (6)$$

where  $R_h^* = \mathbf{f}_h' \mathbf{K}^*$ , and the  $J + 1$  complementary slackness conditions

$$\boldsymbol{\mu}'\mathbf{K}^* \geq \alpha \frac{1}{H} \sum_{h=1}^H E[QD_h], \quad \lambda^* \geq 0, \quad \lambda^*(\boldsymbol{\mu}'\mathbf{K}^* - \alpha \frac{1}{H} \sum_{h=1}^H E(QD_h)) = 0, \quad (7)$$

$$K_j^* \geq K_j^e, \quad \xi_j^* \geq 0, \quad \xi_j^*(K_j^* - K_j^e) = 0 \quad \forall j. \quad (8)$$

The first term in (6) is the sum of the marginal reduction in the expected thermal production cost and the marginal reduction in ancillary services costs associated with an increase in renewable

investment at location  $j$ . The second term is the capital cost of the marginal capacity, and the third term is the marginal value of the expected contribution to achieving the RPS target. The last term is shadow price associated with the constraint that renewable capacity  $K_j^*$  at location  $j$  must be at least equal to existing capacity  $K_j^e$  at that location. It is suboptimal to increase capacity above  $K_j^e$  if the marginal costs dominate the first two effects, in which case  $\xi_j^* \geq 0$  and  $K_j^* = K_j^e$ . Otherwise,  $\xi_j^* = 0$  and capacity at location  $j$  strictly exceeds the existing capacity at that location.

Computing the optimal portfolio of renewable capacity investments assuming that all locations have zero existing capacity simply sets  $K_j^e = 0$  for all  $j$ . For this case,  $\xi_j$  is the shadow cost of installing capacity at location  $j$  when there is no capacity at location  $j$  and it will be equal to zero if the optimal solution installs any capacity at that location.

Different from the case of the thermal cost of meeting the difference between the hourly demand,  $QD_h$ , and hourly renewable output,  $R_h$ , where one can simply integrate under the aggregate thermal cost curve up to the residual demand for thermal energy, there is no straightforward way to compute the ancillary services costs associated with any possible combination of hourly renewable output and system demand. Consequently, we assume a functional form that captures three basic features about the relationship between expected ancillary service costs and the first two moments of system demand and renewable energy production.

We assume that  $A^h(R_h, QD_h) = \frac{\theta}{2}(R_h - QD_h)^2$  for  $\theta > 0$ , where  $R_h = \mathbf{K}'\mathbf{f}_h$ . Taking the expectation of this function we obtain:

$$E[A^h(R_h, QD_h)] = \frac{\theta}{2}[Var(R_h) - 2Cov(R_h, QD_h) + Var(QD_h) + (E[R_h] - E[QD_h])^2]. \quad (9)$$

This functional form captures a number of features of the actual relationship between expected ancillary costs and the first two moments of the joint distribution of hourly renewable output and hourly demand. First, expected ancillary services costs are increasing in the variance of both renewable output and system demand. Second, expected ancillary services costs are decreasing in the covariance between renewable output and demand. Third, ancillary services costs are increasing in the difference between expected renewable output and expected demand. In our empirical application, we econometrically estimate  $\theta$  using using hourly total ancillary services cost and hourly values of  $R_h$  and  $QD_h$  from the California ISO find that the  $\theta$  is positive and precisely estimated.

With this functional form for  $A^h(R_h, QD_h)$ , an expression for the marginal increase in the expected ancillary services cost with respect to an increase in capacity at renewable location  $j$  that enters (6),

$$E\left[\frac{\partial A^h(R_h, QD_h)}{\partial R_h} f_{jh}\right] = -\theta[E[QD_h] - \boldsymbol{\mu}'\mathbf{K}]\mu_j + \theta[\sigma_{jj}K_j + \sum_{i \neq j}^J \sigma_{ij}K_i - cov(f_{jh}, QD_h)],$$

can be expressed in terms of the parameters of the first two moments of the joint distribution of the

vector of hourly locational capacity factors and hourly demand. We now have all of the ingredients necessary to derive the optimal interconnection tariffs for each renewable energy location. The marginal ancillary services cost associated with investment at a particular location  $j$ , all else equal, is small if the variance in output is small, the covariance with output at other locations is small and the covariance with consumption is large. It is small also if the expected output at the location is large. In theory, the marginal ancillary services cost could be negative with this specification.

### 3.3 Optimal Network Interconnection Tariffs

To derive an optimal interconnection tariff, consider the marginal profitability of investing an additional MW at renewable resource location  $j$ :

$$\frac{1}{H} \sum_{h=1}^H E[pr_{jh}f_{jh}] - DF_j - \frac{\partial S^j(\mathbf{K})}{\partial K_j} \Big|_{K_j=K_j^*} + \xi_j^* \quad (10)$$

evaluated at the efficient portfolio  $\mathbf{K}^*$ . The first term is the expected revenue, the second term is the capital cost of the marginal increase in capacity at location  $j$ . The third term is the marginal interconnection tariff at location  $j$ . By subtracting the marginal profitability condition (10) from (6), we can align the marginal private and social incentives if and only if

$$\begin{aligned} \frac{\partial S^j(\mathbf{K})}{\partial K_j} \Big|_{K_j=K_j^*} &= \frac{1}{H} \sum_{h=1}^H E\left[\frac{\partial A^h(R_h^*, QD_h)}{\partial R_h} f_{jh}\right] \\ &+ \frac{1}{H} \sum_{h=1}^H E\left[(pr_{jh} + \frac{\partial C^h(R_h^*, QD_h)}{\partial R_h} - \lambda^*) f_{jh}\right]. \end{aligned} \quad (11)$$

Implementing the social optimum as a decentralized equilibrium requires a network tariff  $S^j(\mathbf{K})$  at location  $j$  that causes investors to internalize the externality associated with the cost of maintaining system stability. This is the first term on the right-hand side of (11). Furthermore, the remuneration  $pr_{jh}$  to renewable electricity production may differ from the marginal social benefit ( $\frac{\partial C^h(R_h^*, QD_h)}{\partial R_h} - \lambda^*$ ) from the investment. If so, the network tariff must also correct this second distortion, which is the term in (11).

Assume that the total hourly price  $pr_{jh}$  paid to renewable resource at location  $j$  is the sum of the wholesale price  $p_{jh}$  and a fixed subsidy  $p\mu_j$  per MWh produced, e.g. a feed-in tariff. Assume also that the wholesale price equals the marginal thermal production cost at every location, so that  $p_{jh} = -\frac{\partial C_h(R_h, QD_h)}{\partial R_h}$ . In that case, the role of the network tariff is to capture the expected marginal ancillary services cost and to correct any distortions associated with the support system

for renewable electricity, which yields:

$$\beta_j = \frac{\partial S^j(\mathbf{K})}{\partial K_j} \Big|_{K_j=K_j^*} = \frac{1}{H} \sum_{h=1}^H E \left[ \frac{\partial A_h(R_h^*, QD_h)}{\partial R_h} f_{jh} \right] + (p\mu_j - \lambda)\mu_j. \quad (12)$$

This expression can be used to implement the efficient portfolio. Assume, for instance, that the annual hourly network tariff for connecting  $K_j$  MW of renewable capacity at location  $j$  to the grid equals

$$S^j(\mathbf{K}) = \frac{\beta_j}{2} \frac{K_j^2}{K_j^*} \quad (13)$$

The expected profit then becomes

$$\frac{1}{H} \sum_{h=1}^H E [pr_{jh} K_j f_{jh}] - K_j DF_j - \frac{\beta_j}{2} \frac{K_j^2}{K_j^*}$$

at location  $j$ , which has a unique solution  $K_j = K_j^*$  if  $K_{-j} = K_{-j}^*$ , where  $K_{-j}(K_{-j}^*)$  is the vector of all other locational (socially optimal) capacity choices besides location  $j$ . The equilibrium network tariff at location  $j$  simply becomes  $\frac{S^j(\mathbf{K}^*)}{K_j^*} = \beta_j/2$  per unit of installed capacity  $K_j^*$ .

## 4 Application to the California Electricity Market

This section presents a stylized application of our modeling framework to the California electricity market. To do this, we require three sets of inputs. First, we need estimates of the first two moments of the hourly joint distribution of  $(\mathbf{f}'_h, QD_h)$  to compute elements of  $E[A^h(R_h, QD_h)]$ , the expected ancillary services cost function. Second, we need the information necessary to compute  $C^h(R_h, QD_h)$ , the total variable cost of meeting the residual demand with thermal units, for each hour of the year. Third, we need information on the realized value of  $A^h(R_h, QD_h)$  and  $R_h$  and  $QD_h$  for a sample of hours to estimate the value of  $\theta$ . Plugging this information into our model allows us to compute the optimal portfolio of renewable generation investments all locations in California to achieve the 33 percent RPS goal.

Before proceeding with this analysis, we would like emphasize that there are many ways to enhance our model to better reflect actual system conditions in California, but these extensions would either significantly complicate the process of solving our model or require additional data we are currently unable to access. We therefore view the application in this section as demonstration of the feasibility and practicality of implementing a locational interconnection charge rather than as finding the correct value for all renewable resource locations in California.

To obtain data on the first two moments of the hourly joint distribution of  $(\mathbf{f}'_h, QD_h)$ , we rely on the data used in Wolak (2016), which contains the hourly capacity factor,  $f_{jh}$  for all 13 solar locations and 40 wind locations producing energy and hourly system demand,  $QD_h$  during the

period April 1, 2011 to March 31, 2012. In terms of the notation of model, the dimension of the vector,  $\mathbf{f}_h$  equals  $J = 53$ . Section 4 in Wolak (2016) presents a comprehensive analysis of the high degree contemporaneous correlation between the hourly renewable energy output at all locations in California. This analysis also demonstrates that the hourly outputs of all solar locations are positively correlated with hourly system demand, whereas the outputs at some wind locations are slightly negatively correlated with hourly system load and others are slightly negatively correlated.

For the second set of data, we have compiled the technical characteristics of all thermal generation units operating in California between April 1, 2011 and March 31, 2012. This information includes the heat rate in millions of BTU (MMBTU) per MWh, the nameplate capacity in MW, and variable operating maintenance costs in dollars per MWh. As shown in Figure 4, all thermal capacity in California is natural gas-fired during this time period.

The heat rate  $HR_g$  of natural gas-fired generation unit  $g$  gives the MMBTUs of natural gas required to produce one MWh of electricity from that unit. We combine this information with the delivered price of natural gas to generation unit  $g$  during day  $d$ ,  $PNATGAS_{gd}$ , for each generation unit during our sample period to compute the variable cost of producing a MWh at thermal generation unit  $g$  during day  $d$  as:

$$VC_{gd} = VOM_g + HR_g \times PNATGAS_{gd},$$

where  $VOM_g$  is the variable operating and maintenance cost of unit  $g$ . we then compute the hourly system-wide marginal cost curve for the time period April 1, 2011 to March 31, 2012, using the value of  $VC_{gd}$  as the height of the step and  $CAP_g$ , the capacity in MW of generation unit  $g$  as the length of the step, for all generation units that are available produce electricity during the hour. Stacking these variable cost and capacity steps from the lowest to highest variable cost yields the system-wide marginal cost curve for hour  $h$  of day  $d$ . Integrating this curve from zero to the level of  $(QD_h - R_h)$ , the residual demand to be served by thermal units, yields the total variable cost of meeting this residual demand.

Although California is currently a significant net importer of electricity, meeting approximately 25 percent of its annual demand from imports, it is likely that it will increasingly export renewable energy during low demand periods with significant in-state renewable energy production. To account for this outcome in our modeling, we allow any excess renewable production in an hour to be sold at the lowest variable cost of any generation unit in California during that hour. Because California relies on incremental imports to meet unexpectedly high demand conditions, we also allow California to meet any shortfall between the production of in-state thermal units the residual demand,  $(QD_h - R_h)$ , from imports at an offer price equal to the highest variable cost unit in California during that hour.

The third dataset is a sample of hourly ancillary services costs, hourly renewable energy production, and hourly system demand that can be used to estimate  $\theta$ , the parameter of our ancillary

services cost function. To estimate this model for the highest currently existing renewable penetration in California, we use data from April 1, 2015 to March 31, 2016, to match the same calendar time period as our other data. During this period there are six ancillary services: Regulation Up, Regulation Down, Spinning Reserve, Non-Spinning Reserve, Regulation Mileage Up, and Regulation Mileage Down. For all of these ancillary services, market participants have the option to self-provide from a generation unit they own or have a contract with. For this reason, we follow the convention used by the California ISO Department of Market Monitoring in reporting ancillary services costs, and take the market price, multiply by the total amount of each ancillary service in that hour (the sum of self-procured capacity and capacity purchased from the market) and multiply that sum by the price. Then we sum these amounts over all the ancillary services to obtain total hourly ancillary services costs.

Annual ancillary services costs were \$62 million in 2015 and \$119 million in 2016. However, as percentage of total wholesale energy purchase costs in the California ISO control area they increased from 0.7 percent to 1.6 percent across the two years.

Table 5 reports the results of estimating the model

$$TAS_{hd} = \alpha_{hd} + \theta(R_h - QD_h)^2 + \epsilon_{hd}, \quad (14)$$

where  $TAS_{hd}$  equals total ancillary services cost during hour  $h$  of day  $d$ ,  $\alpha_{hd}$  denotes different combinations of fixed-effects that vary by hour-of-the-day, day-of-the-week and month-of-the-year and with interactions of these fixed effects. Regardless of which combinations of fixed-effects are used, the estimate of  $\theta$  is virtually unchanged and very precisely estimated. We use a value of  $\theta = 6 \times 10^{-5}$  in solving our model.

The final parameters necessary to solve our model are the dollars per MW of installed capacity cost of building a wind or solar generation unit. There is considerable debate over the precise value of these costs. We use estimates of these figures of \$2,000 per KW for wind from Anderson et al. (2017) and \$4,000 per KW for solar for all locations from recent data compiled from the California Solar Initiative for systems larger than 1 MW.<sup>4</sup> We also assume  $\delta = 1/(1+r)$  for  $r = 0.10$  and a life-span of twenty years,  $\tau = 20$ . The qualitative features of our empirical results are not significantly different for reasonable changes in these magnitudes. Only the value of  $\lambda^*$ , the shadow price on the RPS constraint at the solution, changed with changes in these magnitudes. Higher values of the capacity costs increase  $\lambda^*$ , as does lower values of the discount rate,  $\delta$ .

We now turn to computing two solutions to the efficient expansion of California's renewable generation capacity to meet its 33 percent RPS goal. The first solution assumes that all locations must continue to have at least their current capacity. The second solution only assumes that capacities at all renewable resource locations must be non-negative.

In both cases we solve the Lagrangian (5), in the first case with  $K_j \geq K_j^e$  for all  $j$ , and in

---

<sup>4</sup>[https://www.californiasolarstatistics.ca.gov/reports/cost\\_vs\\_system\\_size/](https://www.californiasolarstatistics.ca.gov/reports/cost_vs_system_size/)

the second case with  $K_j \geq 0$  for all  $j$ . We use the realized variable cost of producing electricity each hour of the year to produce the realized residual demand during that hour,  $C^h(R_h, QD_h)$  in place of  $E[C^h(R_h, QD_h)]$  and the realized value of  $A^h(R_h, Q_h)$  in place of  $E[A^h(R_h, Q_h)]$  in 5. In the RPS constraint we replace  $E(QD_h)$  with the actual value of  $QD_h$ . Finding the solution to (5) requires solving a bound-constrained, nonlinear program with a single linear constraint (the RPS constraint).

To compute the residual demand faced by thermal resources in California each hour we must account for the fact that there are other generation technologies in use besides wind, solar and natural gas-fired generation. As shown in Figure 4, there are also small and large hydroelectric units, biomass, geothermal and nuclear power. Small hydro, biomass, and geothermal production count towards the state's RPS goals. Consequently in computing the RPS constraint, we count the hourly production of these units, which we denote by  $QR_h$ . We also subtract the hourly production of the sum of nuclear units, large hydroelectric units, and net imports which we denote  $QO_h$  to compute the value of  $QD_h$ . In terms of this notation, the RPS constraint in (5) becomes:

$$\frac{1}{H} \sum_{h=1}^H \mathbf{f}_h \mathbf{K} \geq \alpha \left[ \frac{1}{H} \sum_{h=1}^H (QD_h + QO_h) \right] - \frac{1}{H} \sum_{h=1}^H QR_h. \quad (15)$$

This constraint is more representative of how the actual RPS mandate applies and it also reflects the fact that hydroelectric and nuclear units contribute to meeting demand in California.

Comparing our two optimal renewable expansion solutions, we find that the  $K_j \geq 0$  solution requires less total solar and wind generation capacity and yields lower total costs than the  $K_j \geq K_j^e$  solution. Specifically, the  $K_j \geq 0$  solution requires 15,713 MW of wind and solar generation capacity, whereas the  $K_j \geq K_j^e$  requires a total of 17,233 MW of wind and solar capacity, a difference of 1,520 MW, which is less than the installed capacity of wind and solar in our base year of 2011 of 3,539 MW. This result implies that more than half of this installed capacity would remain if California was able to start from zero capacity at all wind and solar locations and meet its RPS goals, but it also suggests that there has been overinvestment at some locations.

The total hourly cost of the  $K_j \geq 0$  solution is \$962,500 per hour, whereas the total cost of the  $K_j \geq K_j^e$  solution is \$1,001,000 per hour, a less than 4 percent increase in costs.

We can compute the optimal locational interconnection charges for each renewable resource location in California as described in the previous section. We consider the case where tariffs are only designed to internalize the increased ancillary services, and does not account for any inefficient subsidies of renewable energy. Consequently,  $\beta_j$  only depends on the first term of (12). To preserve the confidentiality of the renewable energy locations, we are unable to report characteristics of specific locations, but we are able to present plots as a function of features of each location.

All of our marginal interconnection charges are negative, indicating that interconnection charges should be a decreasing function of the volume of installed capacity at that location. This result is

partially driven by our functional form assumption for  $A^h(R_h, Q_h)$  and the fact that the expected demand for solar, wind and thermal units exceeds expected solar and wind output,  $E[Q_h] > E[R_h]$ . We plan to explore richer functional forms for the ancillary services cost functions to see if this result continues to hold. For example, assuming that  $A^h(R_h, Q_h) = \alpha Q_h + \beta R_h + \theta(R_h - Q_h)^2$ , might allow for the possibility of positive marginal interconnection charges.

We first present the histograms of  $\frac{S^j(\mathbf{K}^*)}{K_j^*}$  for all renewable resource locations separately for the  $K_j \geq 0$  and  $K_j \geq K_j^e$  solutions. Figure 5 presents the  $K_j \geq 0$  results and Figure 6 presents the  $K_j \geq K_j^e$  results. The two histograms are quite similar, which is not surprisingly given the similarity of the two optimal solutions.

There is a significant amount of variation in the size of these interconnection payments. Most are in the range of \$0.10/MWh and \$0.25/MWh, which translates into between \$876 per year per MW and \$2,200 per year. As we discussed previously, we expect the absolute value of these magnitudes to change as we refine our modeling effort. They are also likely to become more economically significant as the share of renewables increases and we enrich our model of ancillary services costs.

Figure 7 plots these optimal interconnection charges as a function of the annual average hourly capacity factor at that location for the  $K_j \geq K_j^e$  solutions. Figure 8 plots them as a function of the annual standard deviation of the hourly factor at that location for this same solution. Figures 9 and 10 repeats these same two figures for the  $K_j \geq 0$  solution. Both solutions there is a positive relationship between the mean capacity factor and the magnitude of interconnection subsidy at that location. There is also a positive relationship between the annual standard deviation of the hourly capacity factor at a location and the size of the interconnection subsidy.

## 5 The Cost of Non-Optimal Policies to California

This section compares the cost of alternative policies for attaining California’s 33 percent RPS goals relative to the optimal policy. To determine the potential cost of not pursuing an optimal interconnection policy, we compute the compliance cost for several plausible alternatives.

We consider two different approaches. The first computes the dollar per MW of annual revenue from producing renewable energy at each location valued at the California ISO’s real-time price for that location for all locations in California. We then restrict all new capacity investments to the five highest dollar per MW of annual revenue locations. We run this scenario for both the  $K_j \geq 0$  constraints and the  $K_j \geq K_j^e$  constraints. Specifically, we solve (5) restricting the set of locations where investment can take place to the top five most profitable locations.

Given that locational prices are observable and a number of private companies sell information that allows a prospective investor to estimate fairly accurately the annual output at that the location, the information necessary to executive this RPS compliance path is readily available. We experimented with a larger number than five locations, but found the results were not appreciably different from those obtained with a larger number of locations.

The second expansion scenario assumes that all locations scale up their existing capacity until the 33 percent RPS constraint is met. This solution simply finds the smallest value of  $\gamma$ , a scalar greater than one, such that the modified RPS constraint (15) is satisfied when all values of  $K_j^e$  are multiplied by the  $\gamma$ . We recognize that is an extremely naive expansion strategy, but include it as an upper bound on how costly non-optimal expansion strategies would be.

For the five-most-profitable-locations solution for the  $K_j \geq 0$  constraints, the total hourly cost is \$962,800, which is only slightly higher than the optimal solution for this case. For the  $K_j \geq K_j^e$  constraints case, the total hourly cost is \$1,005,900, which is also higher than the optimal solution for this case. These results support the view that as long as new entrants focus on the most profitable locations, they should be able to come close to the optimal configuration.

This outcome is not guaranteed because the new entrants will have to find the optimal mix of capacity at each of these locations, which is what our optimal interconnection tariffs should deliver. Nevertheless, by restricting attention to just these locations, solutions very close to the social optimum can be found.

It is interesting to note that in terms of installed capacity the solutions that invest only at the five most profitable locations are able to satisfy the RPS goals with less investment in renewable generation capacity than the optimal solutions. For the  $K_j \geq 0$  solution, the five-most-profitable-locations solution requires, 15,627 MW, versus 15,713 MW for the least cost solution. For the  $K_j \geq K_j^e$  solution, the five-most-profitable-locations solution requires 17,200 MW, versus 17,233 MW for the least cost solution.

For the solution that scales up the existing renewable capacity at all locations by the same factor,  $\gamma > 1$  is significantly more expensive and requires much more renewable capacity. The total cost per hour is 1,332,700 dollars and the total amount of installed capacity is 28,790 MW. This result demonstrates that expansion policies that do not consider the factors we discuss can lead to substantially more expensive paths to compliance with the RPS.

## 6 Conclusions

In many regions ancillary services costs have become increasingly important because of the rapid increase in intermittent renewable energy production brought about by renewable energy mandates. The traditional approach to recovering ancillary services costs as a per unit charge on demand may need to be revisited because where renewable generation units locate influences the magnitude of these costs. We propose locational renewable generation interconnection payments as a way to provide incentives for more efficient renewable generation locational decisions.

These payments could reduce or replace traditional renewable support mechanisms that pay per unit of energy produced, such as feed-in tariffs and production tax credits. Instead, renewable resource owners would receive a dollar per MW payment each hour of the year for each MW of capacity interconnected at that location. This would eliminate inefficient renewable production

decisions caused by feed-in tariffs and production tax credits. Renewable resource owners would no longer have an incentive to produce at negative wholesale prices, as they do with the per-MWh-produced incentive schemes. Instead, they would receive the \$/MW payment per hour regardless of how much energy they actually produce and cease production when prices are negative.

Although we are cautious in drawing quantitative conclusions from our stylized empirical analysis, we believe several qualitative conclusions are possible that are likely to hold with a more realistic model. First, we find significant differences across locations in the value of the optimal interconnection payment for California renewable generation locations. Second, the absolute level of the payments is modest, less than one dollar per MW of installed capacity for each hour of the year, but they differ by multiples as high as four to one across California renewable resource locations. These results support the view that interconnections tariff/payments yield a more cost-effective pathway to meeting RPS goals.

## References

- Anderson, John, Gordon Leslie, and Frank A. Wolak**, “Experience and Evolution of Wind Power Project Costs in the United States, <http://www.stanford.edu/~wolak>,” 2017.
- Wolak, Frank A.**, “Level versus Variability Trade-offs in Wind and Solar Generation Investments: The Case of California,” *The Energy Journal*, 2016, 37 (SI2), 185–220.

Table 1: Annual Moments of Hourly Wind, Solar, and Wind and Solar Output (MWh)

	2013	2014	2015	2016
	Hourly Wind Output (MWh)			
Mean	1034.03	1131.52	999.6	1204.8
Standard Deviation	843.15	880.83	822.13	918.27
Coefficient of Variation	0.82	0.78	0.82	0.76
Standard Skewness	0.39	0.49	0.53	0.41
Standard Kurtosis	2.03	2.29	2.18	2.05
	Hourly Solar (MWh)			
Mean	316.58	1005.01	1518.31	1918.71
Standard Deviation	434.74	1286.77	1900.02	2384.97
Coefficient of Variation	1.37	1.28	1.25	1.24
Standard Skewness	1.23	0.85	0.83	0.73
Standard Kurtosis	3.51	2.14	2.65	1.86
	Hourly Combined Wind and Solar Output (MWh)			
Mean	1350.61	2136.53	2517.9	3123.51
Standard Deviation	882.46	1457.94	1977.27	2420.45
Coefficient of Variation	0.65	0.68	0.79	0.77
Standard Skewness	0.19	0.45	0.63	0.55
Standard Kurtosis	2.32	2.5	2.97	2.07

Data Source: California ISO Oasis Web-Site

Table 2: Wind Output Shortfall Durations (Hours)

	2013	2014	2015	2016
Threshold Value	500 MWh			
Number of durations	162	190	199	212
Mean	19.19	14.64	16.35	12.82
Standard Deviation	38.61	28.58	28.06	22.5
Maximum	288	216	209	157
Threshold Value	1000 MWh			
Number of durations	222	263	227	225
Mean	20.06	16.22	21.15	18.43
Standard Deviation	43.47	39.79	44.65	34.52
Maximum	357	430	434	268
Threshold Value	1500 MWh			
Number of durations	255	267	225	262
Mean	23.53	21.78	27.63	20.83
Standard Deviation	49.25	46.68	73.44	38.39
Maximum	374	485	949	290
Threshold Value	2000 MWh			
Number of durations	185	211	193	218
Mean	40	33.75	38.66	30.89
Standard Deviation	94.26	87.82	92.48	58.66
Maximum	856	930	952	399

Data Source: California ISO Oasis Web-Site

Table 3: Solar output Shortfall Durations (Hours)

	2013	2014	2015	2016
Threshold Value	500			
Number of durations	348	367	365	367
Mean	17.61	13.72	13.33	12.93
Standard Deviation	13.94	1.92	1.5	1.78
Maximum	191	21	17	19
Threshold Value	1000			
Number of durations	181	365	365	366
Mean	43.24	14.96	14.01	13.73
Standard Deviation	299.07	2.27	1.68	2.28
Maximum	4041	43	20	42
Threshold Value	1500			
Number of durations	30	359	364	365
Mean	288.23	16.35	14.72	14.27
Standard Deviation	1429.85	4.53	2.24	3.35
Maximum	7858	66	42	67
Threshold Value	2000			
Number of durations	1	330	360	363
Mean	8758	19.35	15.66	14.94
Standard Deviation	0	21.57	3.58	4.79
Maximum	8758	371	44	94

Data Source: California ISO Oasis Web-Site

Table 4: Combined Wind and Solar Output Shortfall Durations (Hours)

	2013	2014	2015	2016
Threshold Value	1000			
Number of durations	230	265	257	225
Mean	13.57	8.34	9.42	8.75
Standard Deviation	27.48	6.13	5.72	5.81
Maximum	288	20	18	21
Threshold Value	2000			
Number of durations	260	388	397	380
Mean	25.54	11.41	10.83	9.63
Standard Deviation	53.44	9.07	5.95	6.53
Maximum	637	82	44	66
Threshold Value	3000			
Number of durations	53	299	356	367
Mean	160.47	21.33	15.84	14.14
Standard Deviation	238.97	42.22	8.57	8.49
Maximum	1283	684	140	141
Threshold Value	4000			
Number of durations	4	191	312	344
Mean	2188	40.06	20.54	16.93
Standard Deviation	1653.46	84.36	30.15	11.69
Maximum	4022	922	501	178

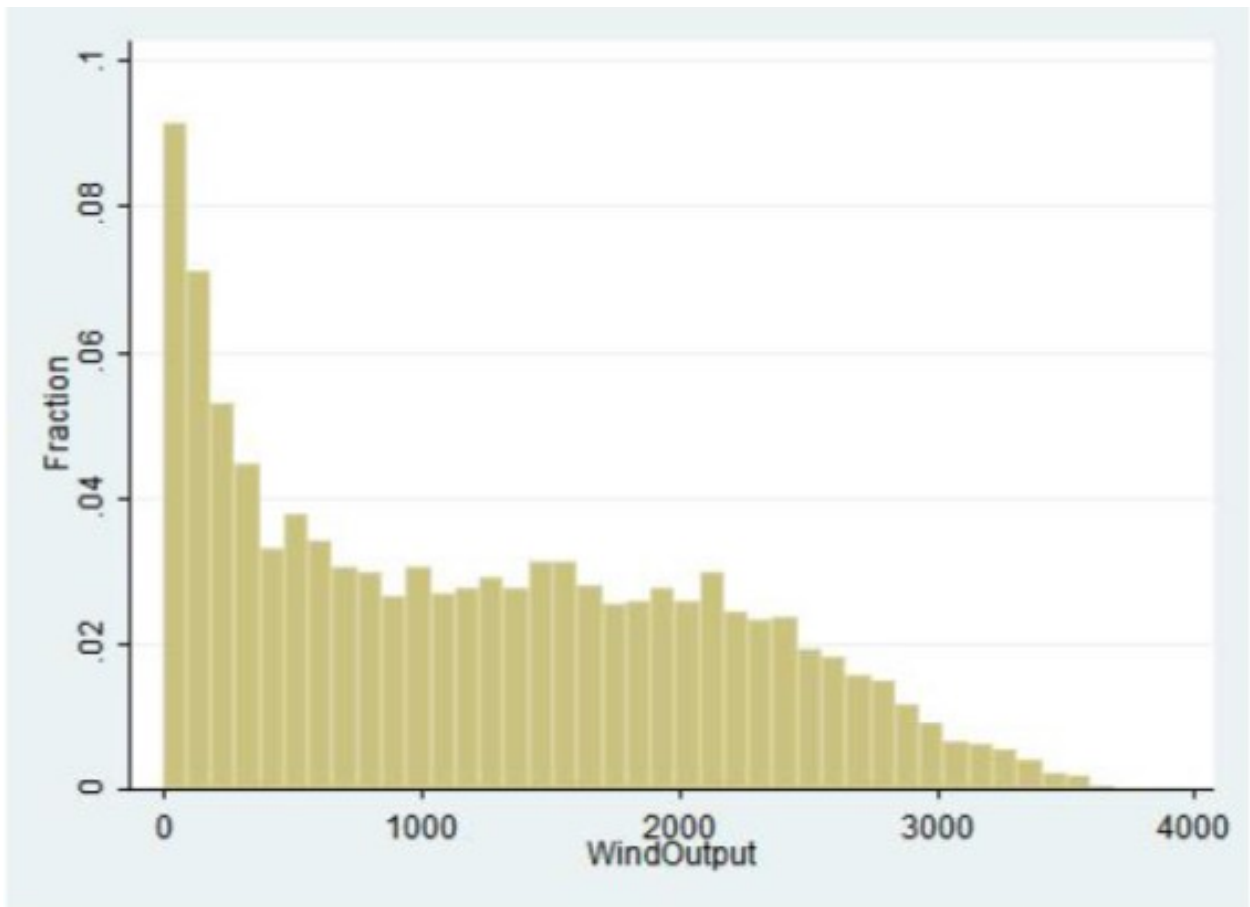
Data Source: California ISO Oasis Web-Site

Table 5: Estimates of  $\theta \times 10^{-5}$

	Total AS Cost / Hour		
$\theta \times 10^{-5}$	6.02	6.08	6.08
Standard Error	(0.137)	(0.164)	(0.164)
Hour, Day of Week, Month FE	Yes	Yes	Yes
Two-way interactions	No	Yes	Yes
Three-way Interactions	No	No	Yes
Observations	8736	8736	8736

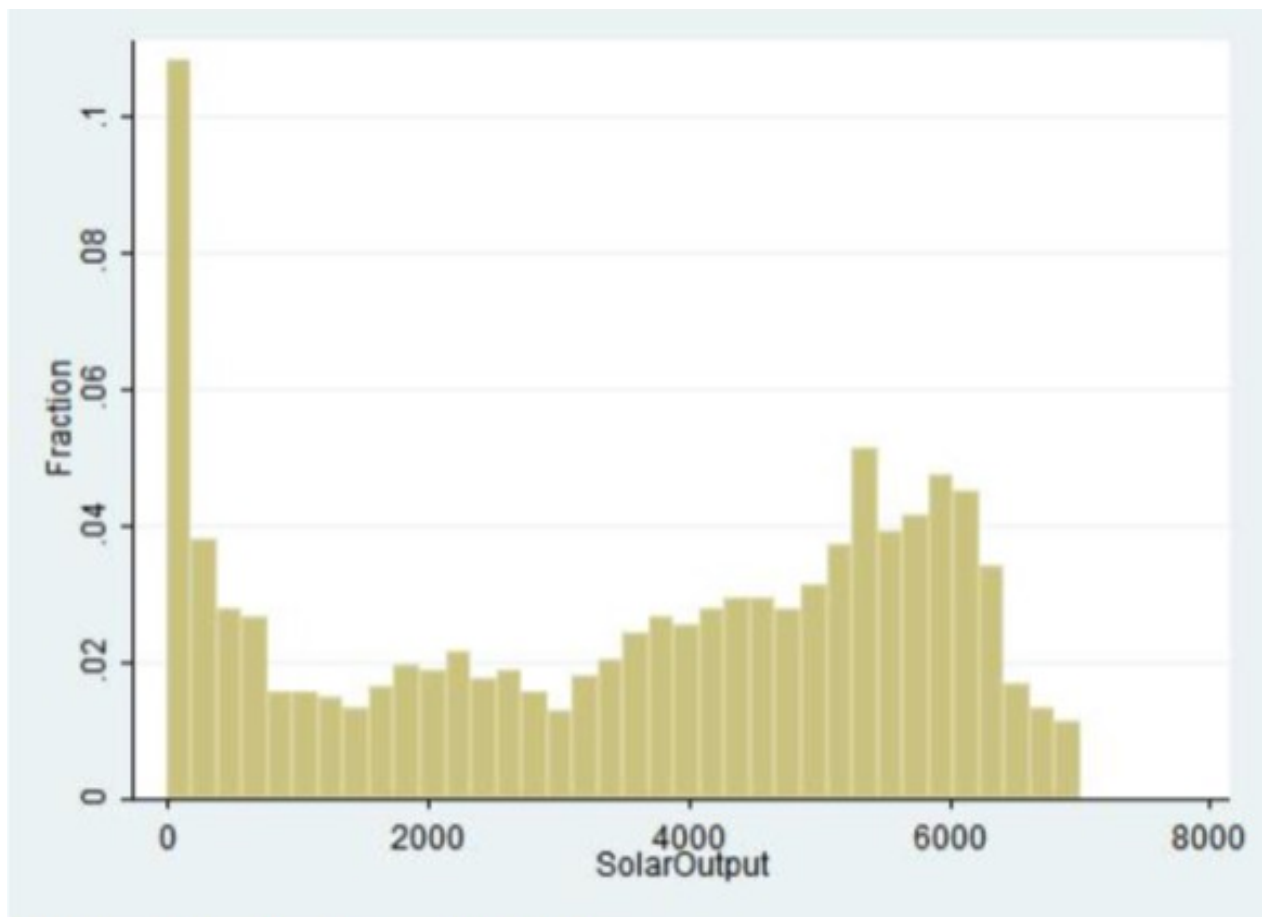
Standard errors in parentheses

FE = Fixed Effects



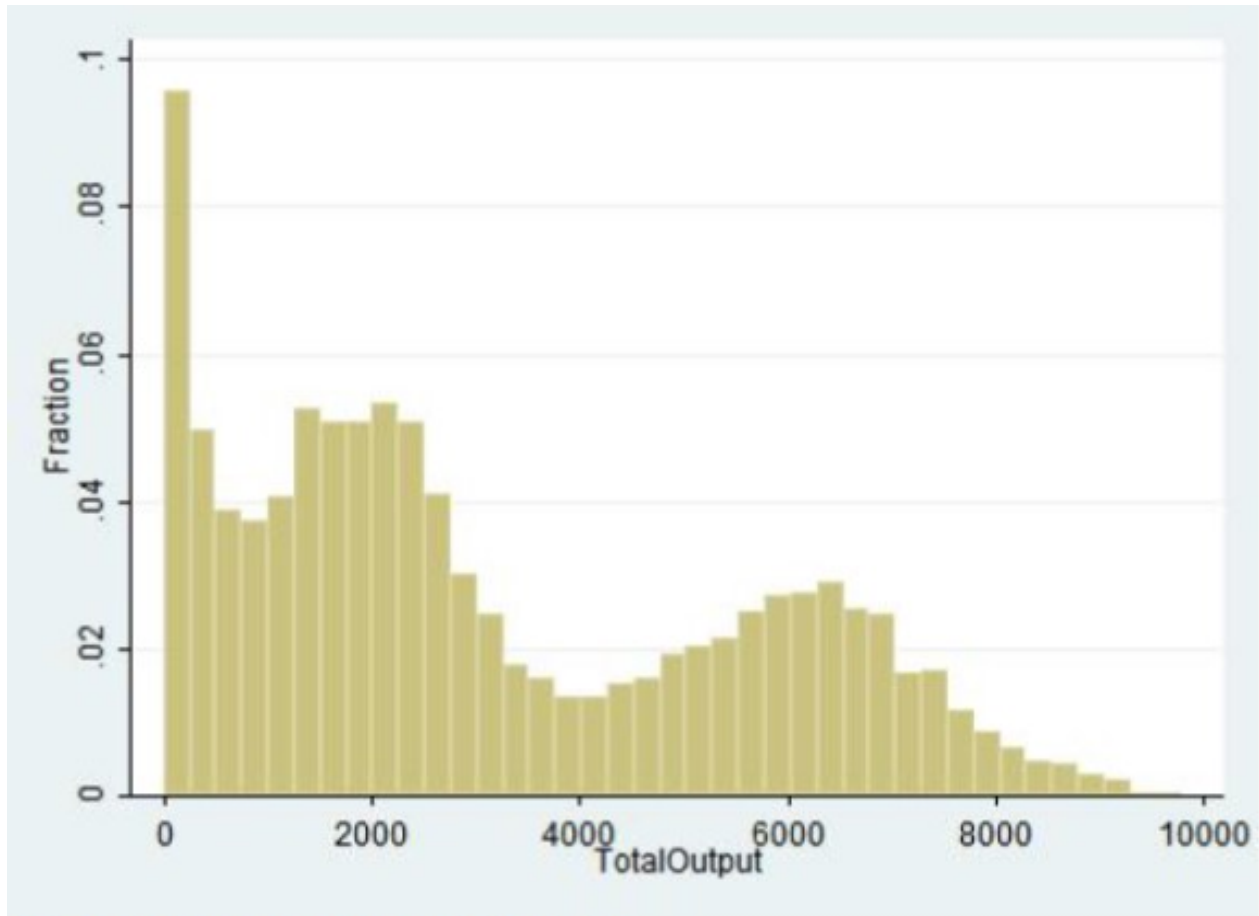
**$P(\text{WindOutput} = 0) = .00967668$**

Figure 1: Histogram of Hourly Wind Output in California ISO Control Area in 2016 (MWh)



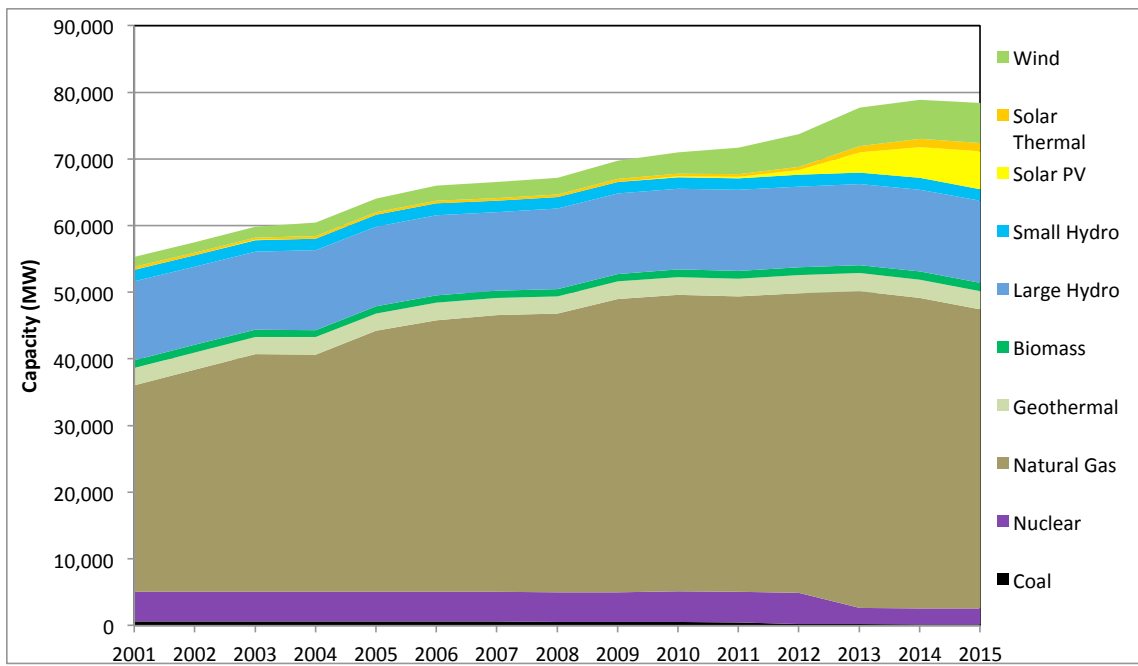
**$P(\text{SolarOutput} = 0) = .45207195$**

Figure 2: Histogram of Hourly Solar Output in California ISO Control Area in 2016 (MWh)



**$P(\text{TotalOutput} = 0) = .00398452$**

Figure 3: Histogram of Hourly Combined Wind and Solar Output in California ISO Control Area in 2016 (MWh)



Source: California Energy Commission, CEC-1304 Power Plant Data Reporting.

Figure 4: In-State Installed Generation Capacity by Technology (MW), Year End 2001 to 2015

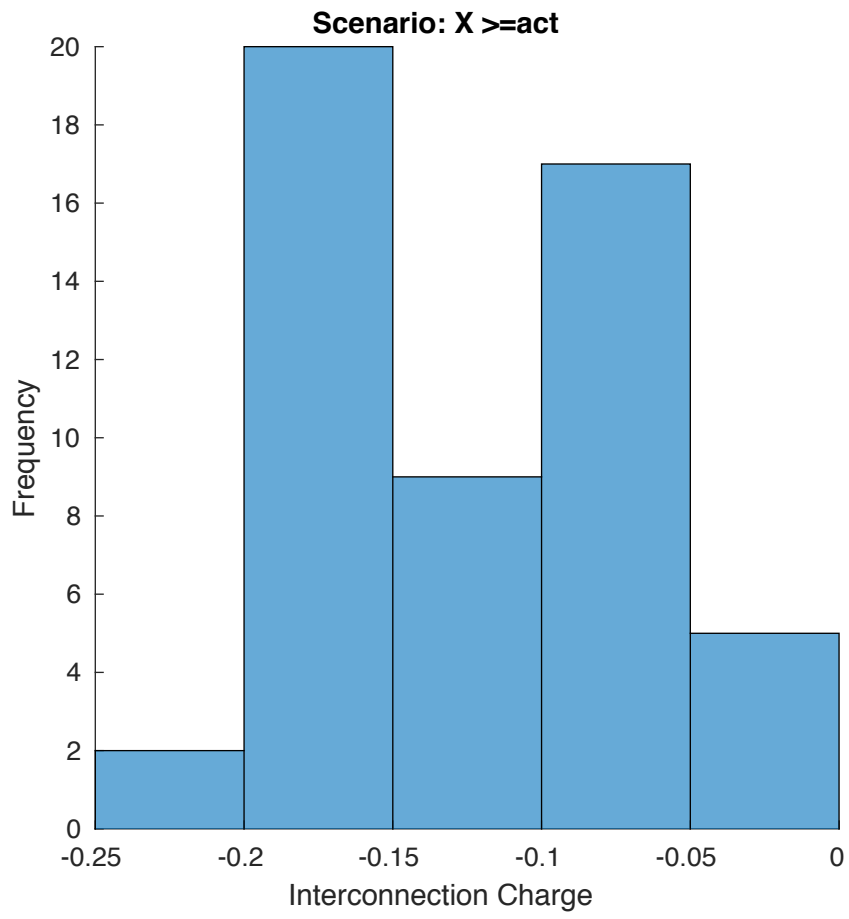


Figure 5: Histogram of Locational Interconnection Charges for the  $K_j^* \geq K_j^e$  Solution

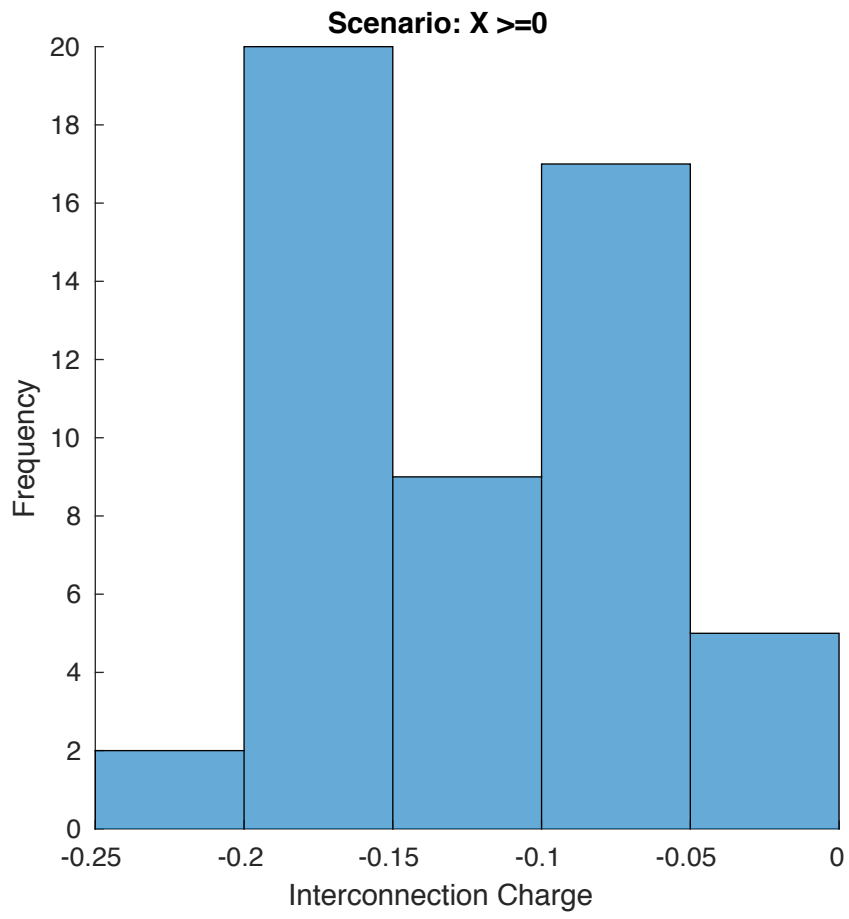


Figure 6: Histogram of Locational Interconnection Charges for the  $K_j^* \geq 0$  Solution

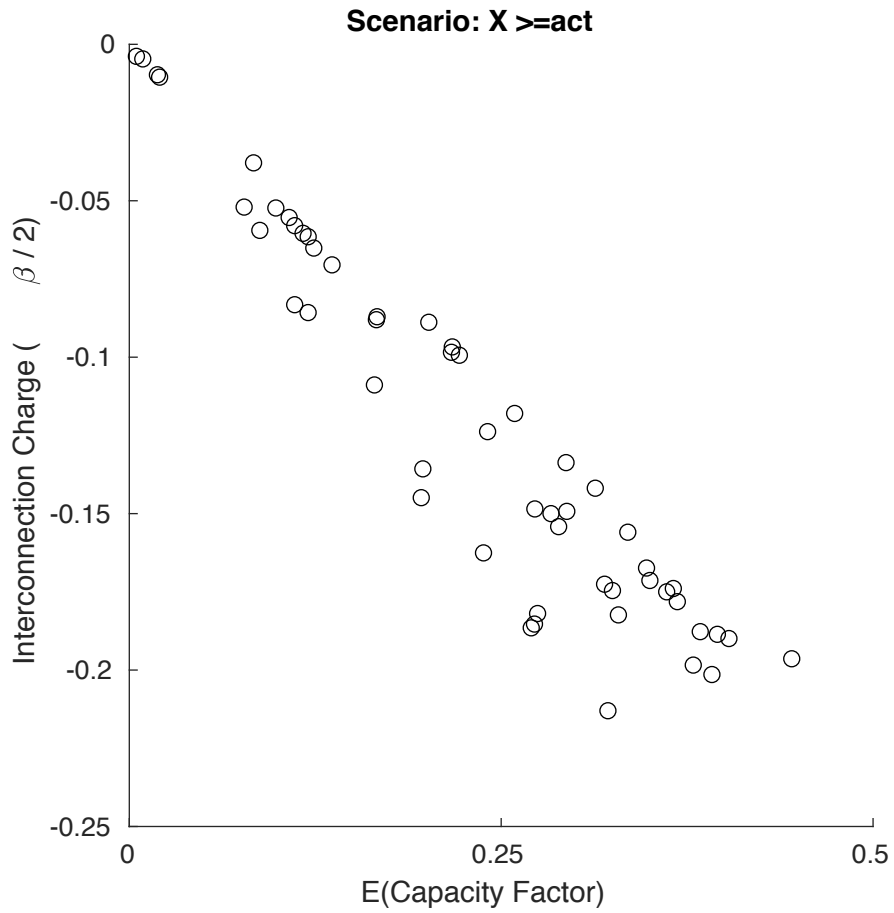


Figure 7: Annual Mean Capacity Factor and Interconnection Charge by Location at the  $K_j^* \geq K_j^e$  Solution

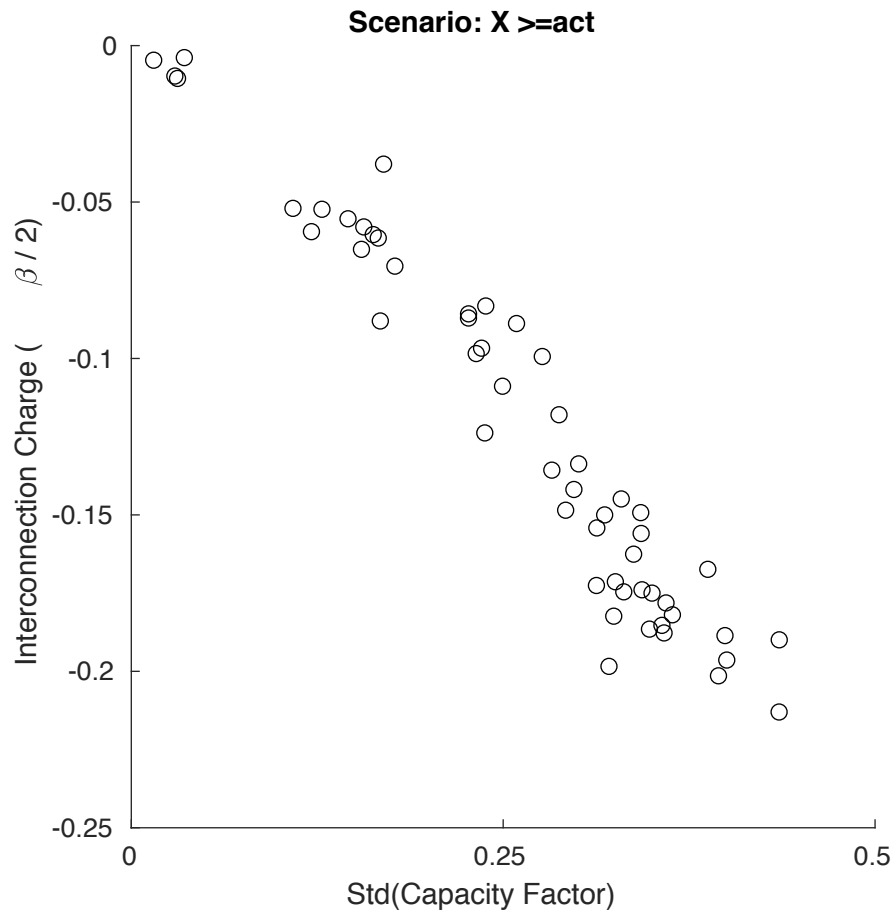


Figure 8: Annual Standard Deviation of Capacity Factor and Interconnection Charge by Location at the  $K_j^* \geq K_j^e$  Solution

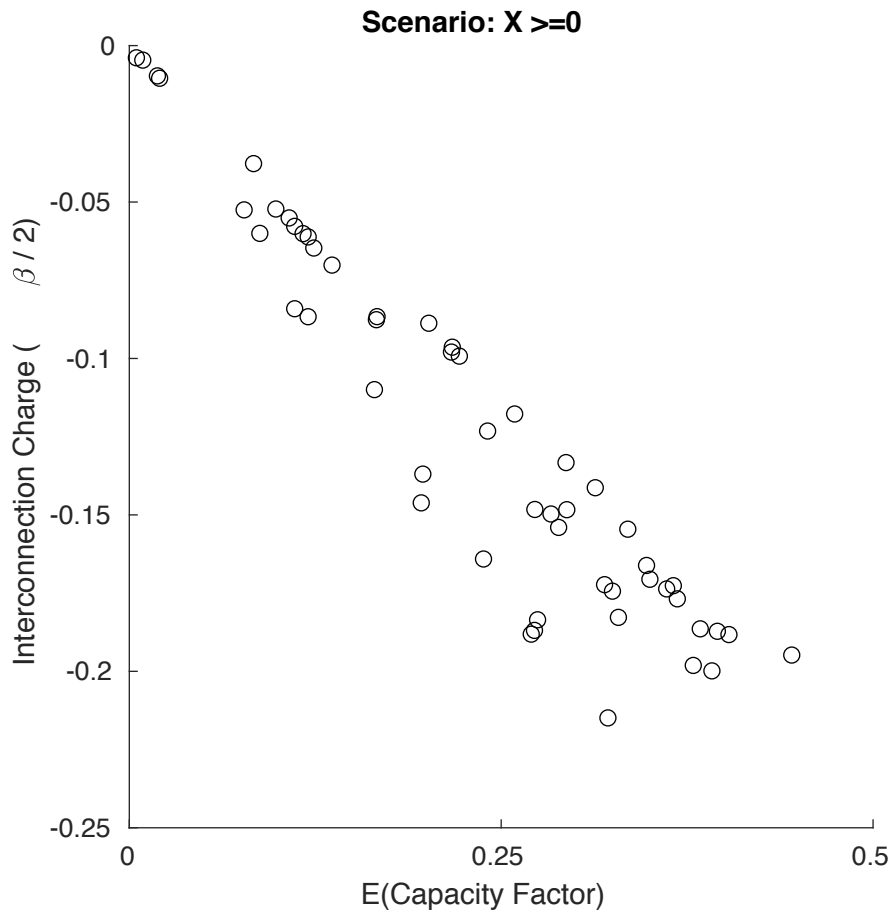


Figure 9: Annual Mean of Hourly Capacity Factor and Interconnection Charge by Location at the  $K_j^* \geq 0$  Solution

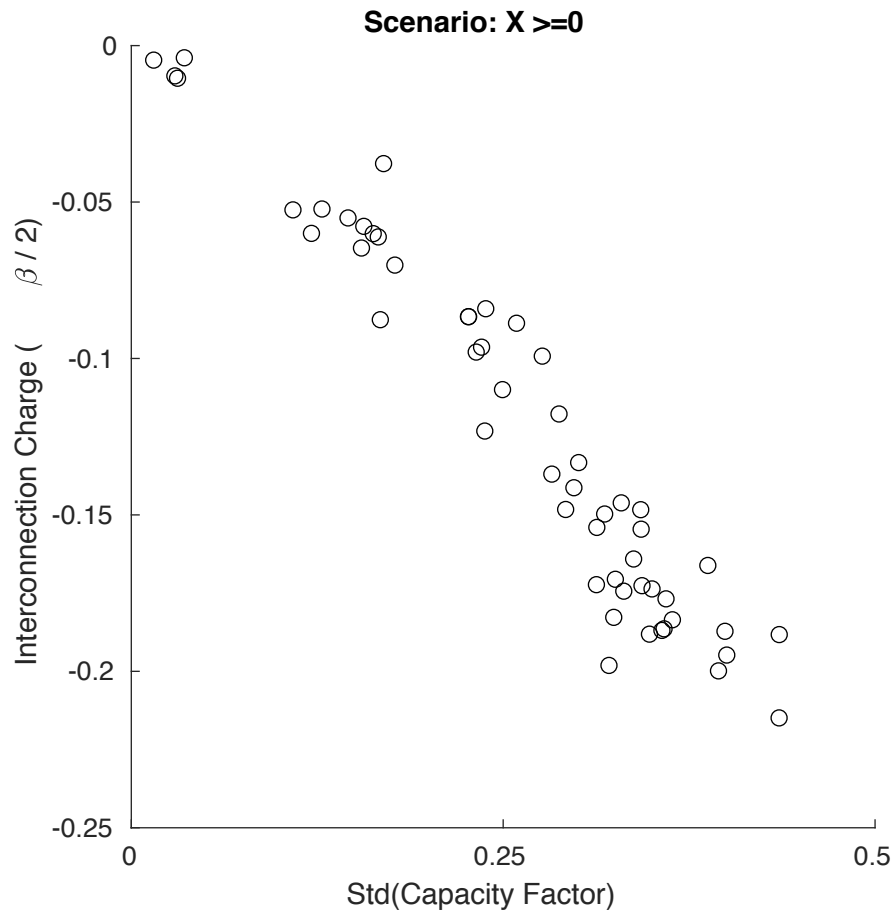


Figure 10: Annual Standard Deviation of Capacity Factor and Interconnection Charge by Location at the  $K_j^* \geq 0$  Solution